

Geometry of chaos in the two-center problem in General Relativity

Ulvi Yurtsever

Jet Propulsion Laboratory 169-327
California Institute of Technology
4800 Oak Grove Drive
Pasadena, CA 91109
and
Theoretical Astrophysics 130-33
California Institute of Technology
Pasadena, CA 91125

December, 1994*

Abstract

The now-famous Majumdar-Papapetrou exact solution of the Einstein-Maxwell equations describes, in general, N static, maximally charged black holes balanced under mutual gravitational and electrostatic interaction. When $N = 2$, this solution defines the two-black-hole spacetime, and the relativistic two-center problem is the problem of geodesic motion on this static background. Contopoulos and a number of other workers have recently discovered through numerical experiments that in contrast with the Newtonian two-center problem, where the dynamics is completely integrable, relativistic null-geodesic motion on the two black-hole spacetime exhibits chaotic behavior. Here I identify the geometric sources of this chaotic dynamics by first reducing the problem to that of geodesic motion on a negatively curved (Riemannian) surface.

*Submitted to Physical Review D

1. The Majumdar-Papapetrou solution

The general Reissner-Nordstrom metric

$$g = - \left(1 - \frac{2M}{r} + \frac{Q^2}{r^2} \right) dt^2 + \left(1 - \frac{2M}{r} + \frac{Q^2}{r^2} \right)^{-1} dr^2 + r^2 (d\theta^2 + \sin^2 \theta d\phi^2)$$

for a charged black hole of mass M and charge Q takes a particularly simple form when the black hole is extremal with $|Q| = M$:

$$g = - \left(1 - \frac{M}{r} \right)^2 dt^2 + \left(1 - \frac{M}{r} \right)^{-2} dr^2 + r^2 (d\theta^2 + \sin^2 \theta d\phi^2) . \quad (1)$$

In the isotropic coordinates $\bar{r} \equiv r - M$, Eq. (1) can be written suggestively as

$$g = - \left(1 + \frac{M}{\bar{r}} \right)^{-2} dt^2 + \left(1 + \frac{M}{\bar{r}} \right)^2 {}^{(3)}\eta , \quad (2)$$

where

$${}^{(3)}\eta = d\bar{r}^2 + \bar{r}^2 (d\theta^2 + \sin^2 \theta d\phi^2)$$

denotes the flat Euclidean metric. The metric function $1 + M/\bar{r}$ appearing in Eq. (2) has the form of a harmonic function in Euclidean space, and, miraculously, when $1 + M/\bar{r}$ is replaced with a more general harmonic function the metric Eq. (2) still remains a solution to the Einstein-Maxwell equations ([1-2]). More precisely, as first discovered by Majumdar and Papapetrou, the metric

$$g = -U^{-2} dt^2 + U^2 (dx^2 + dy^2 + dz^2) \quad (3)$$

and the electromagnetic potential A_a given by

$$A = \pm \frac{1}{U} dt \quad (4)$$

are a solution to the source-free Einstein-Maxwell equations as long as the function $U = U(x, y, z)$ satisfies Laplace's equation in flat space:

$$\sum_{k=1}^3 U_{,kk} = U_{,xx} + U_{,yy} + U_{,zz} = 0 . \quad (5)$$

Note that this solution is static ($\partial/\partial t$ is a timelike Killing vector), but in general has no other symmetries.

It was first realized by Hartle and Hawking ([3]) that with the choice

$$U(\vec{r}) = 1 + \sum_{i=1}^N \frac{M_i}{|\vec{r} - \vec{r}_i|} \quad (6)$$

for the potential $U(x, y, z)$, the Majumdar-Papapetrou solution represents N extremal black holes, where the i 'th black hole, stationary at the fixed position $\vec{r} = \vec{r}_i$, has mass M_i and charge $|Q_i| = M_i$. All charges Q_i have the same sign given by the sign chosen in Eq. (4), which ensures that the holes remain in

equilibrium, balanced under mutual gravitational attraction and electrostatic repulsion. The apparent singularity in $U(x, y, z)$ [and therefore in the metric Eq. (3)] at the positions $\vec{r} = \vec{r}_i$ is the usual coordinate singularity associated with static coordinates at an event horizon. Indeed, the surface area of a small coordinate sphere $\{t = \text{const.}, |\vec{r} - \vec{r}_i| = \epsilon\}$ around $\vec{r} = \vec{r}_i$ approaches the expected surface area of the horizon:

$$\begin{aligned} \lim_{\vec{r} \rightarrow \vec{r}_i} (U^2 4\pi |\vec{r} - \vec{r}_i|^2) &= 4\pi \lim_{\vec{r} \rightarrow \vec{r}_i} \left[\left(1 + \frac{M_i}{|\vec{r} - \vec{r}_i|} + O(1) \right)^2 |\vec{r} - \vec{r}_i|^2 \right] \\ &= 4\pi M_i^2, \end{aligned} \tag{7}$$

and the metric can be extended analytically into the interiors of the black holes (into “negative $|\vec{r} - \vec{r}_i|$ ”) using Kruskal-like coordinates. As in the single black hole case (the extremal Reissner-Nordstrom solution), the interiors of the black holes house true physical singularities where spacetime curvature blows up.

2. Chaos in the two-black-hole spacetime

When $N = 2$, the spacetime given by Eqs. (6) and (3) represents a relativistic analogue to the two-center configuration in Newtonian gravity, in which the Newtonian gravitational field is generated by two point masses at fixed positions (i.e., the mutual gravitational interaction of the masses is ignored). Numerical investigations of null geodesic motion on this two-black-hole spacetime by Contopoulos and coworkers ([4]) have revealed that the geodesics exhibit chaotic behavior in the vicinity of the two centers. More specifically, Contopoulos studies null geodesics whose spatial motion is confined to a two-dimensional symmetry plane; assuming the black holes are positioned along the z -axis, this plane is typically the surface $\{x = 0\}$ (see Fig. 1). Numerical integration of the null geodesic equations then reveals that for geodesics that approach the black holes from infinity, it is essentially impossible to predict whether the orbit will plunge into the first hole, or the second one, or escape back out to infinity; in other words the qualitative behavior of the orbits near the black holes exhibits effectively stochastic features. This places the relativistic two-center motion in surprising contrast with the corresponding Newtonian problem (i.e., the motion of a massive test body in the gravitational field of two fixed centers) where the dynamics is known to be completely integrable (a classical result that goes back to the work of Jacobi and Liouville).

In this paper I will argue that the chaotic behavior of the null geodesic flow has its roots in the spatial geometry of the two-black-hole spacetime, and I will do so by first showing that the dynamics of this flow can be reduced to that of ordinary geodesics on a negatively curved Riemannian surface.

3. Geometric analysis of the two-black-hole null geodesic flow

I will rely on the well-known ‘‘Fermat’s principle’’ in its relativistic formulation ([5]). Fermat’s principle states that if $\mathbf{M} = \mathbf{R} \times \Sigma$ is a static spacetime with metric

$$g = g_{00} dt^2 + {}^{(3)}h ,$$

where Σ is a 3-manifold, and $g_{00} < 0$ is a smooth function and ${}^{(3)}h$ is a Riemannian metric on Σ (both independent of t), then the null geodesics of (\mathbf{M}, g) when projected onto Σ are precisely the Riemannian geodesics of the 3-geometry

$$\left(\Sigma, \frac{{}^{(3)}h}{-g_{00}} \right) ; \quad (8)$$

and, furthermore, the affine parameter (i.e., the arc length) along the projected geodesics in $[\Sigma, {}^{(3)}h/(-g_{00})]$ is precisely the static time coordinate t measured along the null geodesics in (\mathbf{M}, g) . In words that would have sounded familiar to Fermat, the principle states that light follows the path of shortest (or extremal) travel time between two given points in 3-space.

In the multi-black-hole solution given by Eqs. (3) and (6), Fermat’s principle shows that null geodesic flow in the asymptotically flat exterior region (outside the event horizons of the black holes) is equivalent to the Riemannian geodesic flow of the 3-geometry (Σ, h) , with the 3-manifold Σ given by $\Sigma = \mathbf{R}^3 \setminus \{N \text{ points}\}$, and with the Riemannian metric h on Σ given by

$$h \equiv \frac{{}^{(3)}h}{-g_{00}} = \Omega^2(dx^2 + dy^2 + dz^2) , \quad (9)$$

where

$$\Omega = U^2 = \left(1 + \sum_{i=1}^N \frac{M_i}{|\vec{r} - \vec{r}_i|} \right)^2 . \quad (10)$$

In the two-black-hole spacetime, I can assume without loss of generality that the holes are positioned along the z -axis at $\vec{r}_1 = (0, 0, 1)$ and $\vec{r}_2 = (0, 0, -1)$ (see Fig. 1). It is obvious that any two-plane containing the symmetry (z -) axis is a totally geodesic submanifold of Σ . As I will focus on null geodesics which lie (spatially) in such a symmetry plane, which I can assume to be the yz -plane $\{x = 0\}$ as in Fig. 1, by Fermat’s principle the null geodesic flow I need to study is equivalent to the geodesic flow on the two-dimensional Riemannian surface (\mathbf{S}, h) , where $\mathbf{S} = \mathbf{R}^2 \setminus \{(0, 1), (0, -1)\}$, and

$$h = \Omega^2(dy^2 + dz^2) , \quad (11)$$

$$\Omega = \left(1 + \frac{M_1}{\sqrt{y^2 + (z-1)^2}} + \frac{M_2}{\sqrt{y^2 + (z+1)^2}} \right)^2 . \quad (12)$$

Note that the geodesic flow of (\mathbf{S}, h) corresponds, in the original spacetime, only to the null geodesic flow in the exterior of the black holes; null geodesic motion in the interior regions is not covered by this correspondence. This point will become clearer after a closer look at the topology and large-scale geometry of (\mathbf{S}, h) :

Global geometry of the Riemannian surface (\mathcal{S}, h)

Look closely at the behavior of the metric h near the centers, e.g., near $\vec{r} = \vec{r}_1 = (0, 1)$. Introducing Euclidean polar coordinates (R, θ) centered around $\vec{r}_1 = (0, 1)$ (i.e., $R \equiv |\vec{r} - \vec{r}_1|$), I can write the conformal factor Ω in the vicinity of \vec{r}_1 as

$$\Omega = \left(1 + \frac{M_2}{2} + \frac{M_1}{R} + O(R) \right)^2, \quad (13)$$

and similarly I can write

$$h = \left(1 + \frac{M_2}{2} + \frac{M_1}{R} + O(R) \right)^4 (dR^2 + R^2 d\theta^2). \quad (14)$$

Now introduce a new radial coordinate $\rho \equiv M_1^2/R$. Then Eq. (14) becomes

$$\begin{aligned} h &= \left(1 + \frac{M_2}{2} + \frac{\rho}{M_1} + O\left(\frac{1}{\rho}\right) \right)^4 \frac{M_1^4}{\rho^4} (d\rho^2 + \rho^2 d\theta^2) \\ &= \left(1 + O\left(\frac{1}{\rho}\right) \right)^4 (d\rho^2 + \rho^2 d\theta^2). \end{aligned} \quad (15)$$

A similar analysis can be carried out in the vicinity of the other center $\vec{r} = \vec{r}_2$ with the same conclusion, namely that what looks like a singularity at $\vec{r} = \vec{r}_1$ (and similarly near the other center) is in fact an entire asymptotically flat Euclidean region squeezed into a small neighborhood of the “point” $\vec{r}_1 = (0, 1)$ in the coordinate system (y, z) . The global geometry of the surface (\mathcal{S}, h) is then as depicted in Fig. 2 below, with three asymptotically flat regions, one at $\vec{r} \rightarrow \infty$, and two others at each of the centers $\vec{r} \rightarrow \vec{r}_1$ and $\vec{r} \rightarrow \vec{r}_2$. As a corollary, the surface (\mathcal{S}, h) is geodesically complete. This is expected, since by Fermat’s principle the affine parameter (i.e., arc length) along the geodesics of (\mathcal{S}, h) is the static time coordinate t measured along the null geodesics of the two-black-hole spacetime, and static time diverges to infinity at the event horizons of the black holes. In other words, a null geodesic in the two-black-hole spacetime falls into the i ’th black hole if and only if the corresponding Riemannian geodesic in (\mathcal{S}, h) escapes into the asymptotic region $\vec{r} \rightarrow \vec{r}_i$.

Local geometry of the Riemannian surface (\mathcal{S}, h)

The intrinsic geometry of a two-dimensional Riemannian manifold *in the small* is determined completely by the Gaussian curvature K (which is one-half the scalar curvature R). With the metric written in the conformally flat form Eq. (11), K is given by

$$K = -\frac{1}{\Omega^2} \Delta(\log \Omega) \quad (16)$$

$$= \frac{1}{\Omega^4} \left[\Omega^3 \left((\Omega^{-1})_{,yy} + (\Omega^{-1})_{,zz} \right) - \Omega_{,y}^2 - \Omega_{,z}^2 \right], \quad (17)$$

where Δ denotes the scalar Laplacian in the flat metric $dy^2 + dz^2$. It is straightforward to compute K for the surface (\mathcal{S}, h) by simply substituting Ω from Eq. (12) in Eq. (17). The result is a complicated expression, not particularly illuminating in its analytic form (which therefore I will not bother to give). A

plot of the curvature K as a function of the coordinates y, z is given in Fig. 3 (where I chose unit masses $M_1 = M_2 = 1$). It is apparent that K is strictly negative throughout \mathcal{S} (and this is true for all masses $M_1, M_2 > 0$). Both far away from and near the centers (where geometry is asymptotically flat) K approaches zero from below as expected (see Fig. 2).

4. Can chaos in the two-black-hole spacetime be explained solely by the negatively curved geometry of (\mathcal{S}, h) ?

In a Riemannian manifold of arbitrary dimension n , negative sectional curvature causes neighboring geodesics to diverge exponentially ([6,7]). Recall the derivation of this well-known result: If Z denotes a vector field along the geodesic γ , Lie transported by a congruence of neighboring geodesics, then

$$\nabla_{\gamma_*} \nabla_{\gamma_*} Z = R_{\gamma_* Z} \gamma_* , \quad (18)$$

where R_{XY} denotes the curvature operator $\nabla_X \nabla_Y - \nabla_Y \nabla_X - \nabla_{[X,Y]}$. Along γ , an infinitesimal neighboring geodesic can then be defined abstractly as any solution of the ‘‘Jacobi equation,’’ a differential equation along γ derived from Eq. (18). In a parallel-propagated basis $\{E_k\}$ along γ such that $E_n = \gamma_*$, Jacobi’s equation is

$$\frac{d^2 Z^a}{ds^2} = -R^a{}_{nbn} Z^b , \quad (19)$$

where s is the affine parameter. For a two-dimensional Riemannian manifold with Gaussian (\equiv sectional) curvature $K = R_{1212}$, and with $Z \equiv Z^1$, Eq. (19) becomes

$$\frac{d^2 Z}{ds^2} = -K Z . \quad (20)$$

Assuming $K < 0$, and assuming the affine parameter s is small compared to $|K/(dK/ds)|_{s=0}|$, Eq. (20) has generic solutions of the form

$$Z(s) \sim A(s) \exp\left(\int^s \sqrt{-K} ds'\right) + B(s) \exp\left(-\int^s \sqrt{-K} ds'\right) , \quad (21)$$

where $A(s)$ and $B(s)$ are slowly-varying amplitudes. It is clear that negative Gaussian curvature K results in an exponentially diverging $Z(s)$ in general. When $K(s)$ is bounded from above by a negative number, Eqs. (20)–(21) imply that γ (as an orbit in the geodesic flow) has positive Liapunov exponents. Obviously, exponential instability of orbits and positive Liapunov exponents are sufficient conditions for the presence of ‘‘sensitive dependence on initial conditions,’’ the key ingredient of chaos. But are these criteria sufficient to demonstrate that chaotic behavior is indeed present?

To investigate this question, let me briefly consider two examples from Newtonian gravitation. Recall that in classical mechanics, for a Hamiltonian system with Lagrangian function

$$L = \frac{1}{2} \sum_{j,k} a_{jk} \dot{q}^j \dot{q}^k - V(q^i) ,$$

motion on a constant-energy (\equiv constant-Hamiltonian) surface $\{H = E\}$ is equivalent to geodesic motion on a Riemannian manifold, namely on the submanifold $\{V(q^i) < E\}$ of configuration space equipped with the Riemannian metric

$$g_E = [E - V(q^i)] \sum_{j,k} a_{jk} dq^j \otimes dq^k \quad (22)$$

(Hamilton-Jacobi-Maupertius... principle; see [6]). Accordingly, in mathematical analogy with relativistic gravitation, so also in Newtonian gravity test-particle dynamics has a geometric description in terms of geodesic motion. In particular, motion in the Kepler and Newtonian two-center problems can both be described in terms of geodesics on a two-dimensional Riemannian surface, and this description can be put in exactly the same form as in Eqs. (11)–(12), except, of course, in the Kepler case the conformal factor Ω takes the form

$$\Omega = \left(E + \frac{M}{r} \right)^{1/2}, \quad (23)$$

and in the Newtonian two-center problem it has the form

$$\Omega = \left(E + \frac{M_1}{|\vec{r} - \vec{r}_1|} + \frac{M_2}{|\vec{r} - \vec{r}_2|} \right)^{1/2}. \quad (24)$$

Plots of the Gaussian curvature of the metric g_E [Eq. (22)] for the (planar) Kepler and Newtonian two-center problems are shown in Fig. 4. In both plots, E is chosen to be $E = -0.1$ (E is chosen negative so that the geodesic flow describes the motion of bound orbits), and the masses are $M = M_1 = M_2 = 1$. There are no surprises: As both systems are completely integrable with stable closed orbits, one would not expect negative curvature to be the dominant geometric feature. Indeed, in the Kepler case curvature is strictly positive, and in the two-center case it is mostly positive, with a small neighborhood of negative curvature in the vicinity of the centers; this small region of negative K corresponds to directional instabilities the orbits have while passing in between the two centers of attraction. [Note that in contrast with the black-hole surface, the center(s) in the Newtonian case are genuine singularities of the metric g_E ; however, these are not curvature singularities (K remains bounded as $\vec{r} \rightarrow \vec{r}_i$), but rather conical singularities with a mass-independent angle deficit π .]

So far the association between negative Gaussian curvature on the one hand and chaotic behavior of the geodesic flow on the other appears to hold within the context of the three examples I discussed. Consider, however, one more example, this time the geodesic flow on the Riemannian surface \mathcal{S} with only one extremal (Reissner-Nordstrom) black-hole; in other words with metric h given by Eq. (11) where $\Omega = (1 + M/r)^2$. The Gaussian curvature K of the resulting geometry is plotted in Fig. 5 (with $M = 1$). As in the two-black-hole case (Fig. 3), K is strictly negative everywhere. But the geodesic flow on this surface is a completely integrable system (angular momentum provides the second integral of motion). Clearly, then, negative curvature (sensitive dependence on initial conditions) is *not* sufficient for chaos: In fact, the unique closed (unstable) geodesic in the geometry of Fig. 5 has strictly positive Liapunov exponents

as an orbit in the flow, so even the presence of positive Liapunov exponents does not always imply chaotic behavior.

As others have done before, I would like to argue in this paper against the widespread practice in the physics literature of identifying chaos with merely the presence of positive Liapunov exponents. This is especially important in relativity (where there is no canonical choice for dynamical time) since whether or not a Liapunov exponent is positive depends crucially on the nature of the time parameter used in defining the exponent. In the next section I will describe a precise formulation for “chaos” [due to S. Willard ([8])] which I believe is particularly useful in relativity since it does not depend sensitively on the choice of time. In the following section (Sect. 6), I will demonstrate that null geodesic flow in the two-black-hole spacetime is chaotic according to this formulation.

5. A precise formulation of chaos

Central to our intuitive understanding of chaotic behavior is the notion of “sensitive dependence on initial conditions:” long-time prediction of motion in the phase space of a chaotic system is impossible since small initial perturbations of the orbits grow arbitrarily large as the system evolves in time. This, of course, is a vague idea in need of a precise mathematical formulation, and there exist various such formulations, the concept of Liapunov exponents being one of them. However, the exact content of our intuitive notion of sensitive dependence is not fully captured by the more precise concept of positive Liapunov exponents. For example, the phase flow $\{\dot{x} = x, x \in \mathbf{R}^n\}$ has positive Liapunov exponents along all its orbits, but, clearly, this is not a chaotic system, and more complicated “counterexamples” with positive exponents can be found in which to discern that motion is non-chaotic would not be so easy. In order to conclude, on the basis of the presence of positive Liapunov exponents, that chaos is present, it is apparently necessary to make sure that the divergence of nearby orbits does not occur simply because these orbits escape to “infinity” under time evolution. What is needed to address this point is a mathematical formulation slightly more sophisticated than the concept of Liapunov exponents.

Here, then, is my favorite “definition” of chaos, adopted from [8]: Restrict attention, for definiteness, to phase spaces \mathbf{M} with metrizable topology. A dynamical system (\mathbf{M}, φ_t) is chaotic if it contains a “chaotic invariant subset,” that is, a subset $\Lambda \subset \mathbf{M}$ such that:

- (C1) Λ is compact, and invariant under φ_t , i.e., $\varphi_t(\Lambda) \subset \Lambda \quad \forall t \in \mathbf{R}$.
- (C2) Λ has sensitive dependence on initial conditions.
- (C3) Λ is topologically transitive.

The precise meaning of condition C2 (sensitive dependence on initial conditions) is the following: Fix a distance function ρ on \mathbf{M} compatible with \mathbf{M} 's topology. Condition C2 holds if there exists a fixed $\delta > 0$ such that for all $x \in \Lambda$ and for every neighborhood $U \subset \Lambda$ of x open in Λ , a point $y \in U$ and a $t > 0$ can be

found such that

$$\rho[\varphi_t(x), \varphi_t(y)] > \delta .$$

In other words, given any point $x \in \Lambda$, no matter how small a neighborhood U of x I choose I can always find points $y \in U \cap \Lambda$ whose orbits eventually diverge away from that of x under the flow φ_t . Since Λ is compact, this notion of sensitive dependence on initial conditions is independent of the choice of ρ . Topological transitivity of Λ (condition C3) means the following: for every open $U, V \subset \Lambda$ there exists a $t \in \mathbf{R}$ such that $\varphi_t(U) \cap V \neq \emptyset$.

Because the problem I study in this paper involves chaos “localized” in a bounded region of an asymptotically flat geometry (i.e., in the vicinity of the black holes), I will need to use a slightly generalized version of the above definition; my generalization is designed to be adapted to the essentially time-asymmetric nature of the problem (i.e., null geodesics approaching the black-hole region from infinity and plunging into the holes after exhibiting chaotic behavior). Namely, call a subset $\Lambda \subset \mathbf{M}$ a “chaotic future-invariant set” if

- (FC1) Λ is compact, and future-invariant under φ_t , i.e., $\varphi_t(\Lambda) \subset \Lambda \quad \forall t > 0$.
- (FC2) Λ has sensitive dependence on initial conditions (defined as before).
- (FC3) Λ is topologically future-transitive.

Note that topological transitivity of Λ as defined above (condition C3) ensures essentially that the flow is topologically “mixing;” this condition is designed to rule out situations in which Λ can be decomposed into multiple compact invariant sets. Clearly, topological transitivity would be an inappropriately strong condition to impose on a subset which is only future-invariant. Therefore, I modify this condition so as to demand that the flow on Λ is mixing only in the future direction, more precisely, I define Λ to be topologically future-transitive if there exists a time $T > 0$ such that for every pair of open subsets $U, V \subset \varphi_T(\Lambda)$ times $t > 0$ and $s > 0$ can be found such that $\varphi_t(U) \cap \varphi_s(V) \neq \emptyset$. Clearly, a chaotic invariant set is also trivially a chaotic future-invariant set. The definition of a chaotic system can now be generalized to include any dynamical system which contains a chaotic future-invariant subset.

Notice that this definition for chaos makes no reference to Liapunov exponents; in fact, the rate of divergence of nearby orbits is not constrained in any way by the precise notion of sensitive dependence on initial conditions. This fact makes the definition especially interesting for applications in General Relativity: sensitive dependence as defined above holds for one choice of time function if and only if it holds for any other, as long as two choices of time are always related by a monotone-increasing diffeomorphism from the real axis \mathbf{R} onto \mathbf{R} . Of course, in general a mathematical definition is useful only if it is the subject of theorems, and there do exist theorems which demonstrate that many of the usual properties of chaotic systems can be derived from the above conditions C1–C3 (or FC1–FC3); I will not discuss these results here, but direct the reader to the literature, especially as listed in [8]. Instead I will turn now to the demonstration that the geodesic flow on the two-surface (\mathbf{S}, h) (which, as I

discussed in Sect. 3, is equivalent to the null geodesic flow of the two-black-hole spacetime) is chaotic according to the formulation of chaos I just described. It is important to note here that other studies (see [9]–[10] and references therein) have carried out this demonstration by searching for various more direct signatures of chaos in the two-black-hole geodesic flow; for instance, the existence of hyperbolic cycles and transverse homoclinic orbits in this flow is discussed in [9], and the presence of positive Liapunov exponents is explored in [10].

6. “Proof” of chaos in the two-black-hole null geodesic flow

The geodesic flow on the Riemannian surface (\mathbf{S}, h) can be described as a Hamiltonian dynamical system, with phase space $\mathbf{M} =$ the unit cotangent bundle of \mathbf{S} , i.e.,

$$\mathbf{M} = T_1^*\mathbf{S} \equiv \{(x, p) \in T^*\mathbf{S} \mid \|p\| = h^{ab}p_a p_b = 1\}, \quad (25)$$

and with the Hamiltonian function $H(x, p) = \frac{1}{2}h^{ab}p_a p_b$. I will denote the geodesic flow on $T_1^*\mathbf{S}$ by the usual symbol φ_t . I showed in Sect. 3 that (\mathbf{S}, h) has strictly negative Gaussian curvature, and recalled in Sect. 4 that negative curvature causes exponential divergence of the orbits in the geodesic flow. Now, if the surface \mathbf{S} were compact, I could then simply define my invariant set Λ to be the entire phase space $\mathbf{M} = T_1^*\mathbf{S}$: so chosen, Λ is compact when \mathbf{S} is, and because of the negatively curved geometry of (\mathbf{S}, h) , Λ has sensitive dependence on initial conditions, i.e., satisfies condition C2 as formulated in the previous section. It is not difficult to show also that Λ is topologically transitive under the geodesic flow; therefore, if \mathbf{S} were compact, all conditions C1–C3 for a chaotic invariant subset would be satisfied by this simple choice of Λ , i.e., the entire phase space would be a chaotic invariant set. Indeed, it is well known that geodesic flows of compact manifolds with negative sectional curvature are chaotic. (These flows in fact satisfy every criteria ever invented for chaos: they have positive Liapunov exponents, positive entropy, are mixing, are K-flows, . . . See [7] for an extensive but readable analysis of this classical problem.) The noncompactness of the two-black-hole Riemannian surface (\mathbf{S}, h) is then the main difficulty I need to overcome in demonstrating the existence of a chaotic (future-) invariant subset in the (noncompact) phase space $T_1^*\mathbf{S}$.

I will now construct a closed subset $\Lambda \subset T_1^*\mathbf{S}$ which I claim is a chaotic future-invariant set for the geodesic flow. That Λ is compact and future-invariant will be evident from its construction, however, I will not be able to prove that Λ satisfies conditions FC2 and FC3. To prove these conditions, it would be sufficient to combine the negatively curved geometry of (\mathbf{S}, h) with the intricate topological structure that Λ appears to have; however, I cannot prove that Λ indeed has this intricate structure. As is usually the case with studies of chaotic behavior, the evidence for this structure is exclusively numerical. Some of this numerical evidence I will present here, and more of it can be found in the literature, e.g., in [4] and [10].

First define subsets Γ_1 , Γ_2 and Γ of the phase space $T_1^*\mathcal{S}$ as follows: Γ_i is the set of all points in $T_1^*\mathcal{S}$ which fall into the i 'th black hole as $t \rightarrow \infty$, i.e.,

$$\Gamma_i \equiv \{m \in T_1^*\mathcal{S} \mid \vec{r}[\varphi_t(m)] \rightarrow \vec{r}_i \text{ as } t \rightarrow \infty\}, \quad (26)$$

and Γ is the set of all points which escape to the asymptotically flat region $\vec{r} = \infty$ as $t \rightarrow \infty$, i.e.,

$$\Gamma \equiv \{m \in T_1^*\mathcal{S} \mid \vec{r}[\varphi_t(m)] \rightarrow \infty \text{ as } t \rightarrow \infty\}. \quad (27)$$

Since these subsets consist of points (x, p) such that the geodesic starting at x with initial tangent vector p eventually escapes to one of the three asymptotically flat regions of (\mathcal{S}, h) (see Fig. 2), it is clear that both the Γ_i and Γ are open subsets in $T_1^*\mathcal{S}$. Also (and this will be important below), it is clear that Γ , Γ_1 and Γ_2 are mutually disjoint subsets, i.e.,

$$\Gamma \cap \Gamma_i = \Gamma_1 \cap \Gamma_2 = \emptyset.$$

Now define Δ as the closed subset

$$\Delta \equiv \text{complement}(\Gamma \cup \Gamma_1 \cup \Gamma_2) = (\Gamma \cup \Gamma_1 \cup \Gamma_2)'; \quad (28)$$

Δ is the set of all points which do not escape to any asymptotic region as $t \rightarrow \infty$, i.e., the set of all future-imprisoned (e.g., periodic or quasi-periodic) orbits of the geodesic flow. This is obviously a future-invariant subset, but it is not necessarily compact (unless all imprisoned orbits are closed geodesics, which is not the case as numerical studies show). To cut Δ down to a compact size, introduce a compact subset $D \subset \mathcal{S}$ as follows (see Fig. 6): Draw a circle \mathcal{C} in the asymptotically flat region $\vec{r} \rightarrow \infty$ which encloses both black holes, and draw circles \mathcal{C}_1 and \mathcal{C}_2 in the asymptotic regions $\vec{r} \rightarrow \vec{r}_1$ and $\vec{r} \rightarrow \vec{r}_2$ which enclose the black holes 1 and 2, respectively. Choose these circles large enough so that if \vec{n} denotes the outward normal to \mathcal{C} and \mathcal{C}_i , a geodesic γ which crosses any one of the circles in the outward direction [i.e., with $h(\gamma_*, \vec{n}) \geq 0$] escapes to the corresponding infinity (and thus never crosses \mathcal{C} or \mathcal{C}_i again). By asymptotic flatness, it is clear that such circles \mathcal{C} and \mathcal{C}_i can be found (see Fig. 6). Now let $D \subset \mathcal{S}$ be the compact region bounded by the circles, in other words, define D to be the unique connected component of $\mathcal{S} \setminus (\mathcal{C} \cup \mathcal{C}_1 \cup \mathcal{C}_2)$ such that $\partial D = \mathcal{C} \cup \mathcal{C}_1 \cup \mathcal{C}_2$. Then put

$$\Lambda \equiv \Delta \cap T_1^*D. \quad (29)$$

So constructed, Λ is clearly both compact (a closed subset of a compact set) and future-invariant. I claim that this $\Lambda \subset T_1^*\mathcal{S}$ is a chaotic future-invariant subset for the geodesic flow on $T_1^*\mathcal{S}$.

As I mentioned above, I am not able to prove that Λ satisfies the conditions FC2 and FC3 of Sect. 5. Nevertheless, a great deal of insight into the structure of Λ can be obtained by numerically integrating the geodesic equations on (\mathcal{S}, h) . Extensive numerical studies of this kind have been reported in [4] and [10]. Although I will base the following observations on my own minimal

investigation of the (numerical) structure of Λ , these observations are supported by the more extensive numerical evidence already published in the literature.

Because of the exponential instability of all orbits in the geodesic flow, it is clear that a direct computer proof of the existence of a future-imprisoned orbit (lying in Λ) is impossible: any real orbit in the computer will eventually diverge away from Λ because of numerical instabilities, even if initially it lies in Λ . So it might appear at first that by relying on numerical integration it is impossible to even prove that Λ is nonempty! This is not the case, however; numerical integration does yield an indirect proof that orbits which lie in Λ exist. More precisely, consider those orbits whose starting points are on the z -axis and whose initial (unit) tangent vectors are entirely in the y -direction. [See Fig. 7; all orbits plotted in Fig. 7 are of this kind. Also, although the orbits plotted in Fig. 7 are (mostly) with unit masses $M_1 = M_2 = 1$ and (some) with masses $M_1 = 2, M_2 = 1$, similar behavior is observed with all positive choices of M_1, M_2 .] In the following, I will not make any distinction between points on the z -axis and initial conditions for the orbits in $T_1^*\mathcal{S}$; the initial-tangent-vector part of the initial conditions is fixed throughout to be a unit vector in the y direction. Now, by numerically integrating these orbits into the future, the following features can be observed: (i) Consider any open interval of initial conditions (starting points) on the z -axis lying in the vicinity of the centers. No matter how small this interval is, there are always points in it which belong to Γ, Γ_1 and Γ_2 . (ii) In any such interval, between any two points that belong to a distinct pair of the subsets Γ, Γ_1 and Γ_2 , there exists a third point which belongs to the subset other than the two in the pair.

Note that since Γ, Γ_1 and Γ_2 are open sets, both of the statements (i) and (ii) are “stable” numerically, i.e., they can be verified with arbitrarily-high-accuracy numerical calculations. Already, the statement (i), combined with the observation that Γ and Γ_i are disjoint, proves that Λ is nonempty: a connected open interval in \mathbf{R} cannot be the union of three disjoint open subsets, therefore, in any interval of the kind described in (i) there must exist points which belong to Λ . As I remarked above, to prove that Λ satisfies the conditions FC2 and FC3 of Sect. 5, it is sufficient to combine the exponential instability of the geodesic flow on $T_1^*\mathcal{S}$ with the everywhere-dense topological structure of Λ , i.e., the structure of a Cantor set of periodic or quasi-periodic orbits, so that every open neighborhood of any point $m \in \Lambda$ contains points of Λ other than m . That Λ indeed has this structure is strongly suggested by the numerical evidence discussed here and more extensively in [4] and [10]. However, the discovery of an analytical proof of this topological structure remains an open problem.

Acknowledgements

This research was carried out at the Jet Propulsion Laboratory, Caltech, and was sponsored by the NASA Relativity Office and by the National Research Council through an agreement with the National Aeronautics and Space Administration.

REFERENCES

1. S. D. Majumdar, Phys. Rev. **72**, 390 (1947).
2. A. Papapetrou, Proc. R. Irish Acad. **A51**, 191 (1947).
3. J. B. Hartle and S. W. Hawking, Commun. Math. Phys. **26**, 87 (1972).
4. G. Contopoulos, Proc. R. Soc. London **A431**, 183 (1990); **435**, 551 (1991).
See also S. Chandrasekhar, Proc. R. Soc. London **A421**, 227 (1989).
5. C. W. Misner, K. S. Thorne and J. A. Wheeler, *Gravitation* (Freeman, San Francisco 1973).
6. V. I. Arnold, *Mathematical Methods of Classical Mechanics* (Springer-Verlag, New York 1978).
7. V. I. Arnold and A. Avez, *Ergodic Problems of Classical Mechanics* (Addison-Wesley, Redwood City 1989).
8. S. Willard, *Introduction to Applied Nonlinear Dynamical Systems and Chaos* (Springer-Verlag, New York 1990).
9. Y. Sota, S. Suzuki and K. Maeda, Waseda University Preprint, 1994.
10. C. P. Dettmann and N. E. Frankel, Phys. Rev. D **50**, R618 (1994).

FIGURE CAPTIONS

Figure 1. Contopoulos’s (and also this paper’s) analysis of the two-black-hole null-geodesic flow is confined to those null geodesics which lie in a two-dimensional surface of symmetry such as the yz -plane $\{x = 0\}$.

Figure 2. The geometry of the Riemannian manifold (\mathcal{S}, h) in the large. Note that this is *not* the actual geometry of the surface $\{x = 0\}$ in the physical metric g on the two-black-hole spacetime, but, rather, it is the physical geometry with an extra conformal factor introduced in accordance with Fermat’s principle. In particular, only the asymptotic region $\vec{r} \rightarrow \infty$ corresponds to the usual asymptotic region in the physical spacetime; the asymptotic regions $\vec{r} \rightarrow \vec{r}_i$ exist because of the singular behavior of the static time coordinate t at the event horizons of the black holes. Accordingly, a null geodesic in the two-black-hole spacetime falls into the i ’th black hole if and only if the corresponding Riemannian geodesic in (\mathcal{S}, h) escapes into the asymptotic region $\vec{r} \rightarrow \vec{r}_i$.

Figure 3. The Gaussian curvature K of the Riemannian surface (\mathcal{S}, h) as a function of the coordinates (y, z) . The masses are chosen to be $M_1 = M_2 = 1$ for this plot; but the qualitative features of K are identical for all positive masses. In particular, K is strictly negative throughout \mathcal{S} , and approaches zero in all three asymptotic regions, i.e., both as $\vec{r} \rightarrow \infty$ and as $\vec{r} \rightarrow \vec{r}_i$, $i = 1, 2$.

Figure 4. No surprises in Newtonian gravity for the connection between negative curvature and chaotic geodesic motion: With completely integrable geodesic flows, Gaussian curvature of the metric g_E [Eq. (22)] is positive for both the Kepler problem (plot on the left; strictly positive K) and the Newtonian two-center problem (plot on the right; K positive except in a small neighborhood of the centers).

Figure 5. The Riemannian surface \mathcal{S} with the metric corresponding to the null geodesic flow of a single extremal Reissner-Nordstrom black hole has strictly negative Gaussian curvature, and the Liapunov exponent of its (unique) closed geodesic is positive. But there is no trace of chaos here: with angular momentum as the second integral of motion, the geodesic flow of this surface is a completely integrable Hamiltonian system.

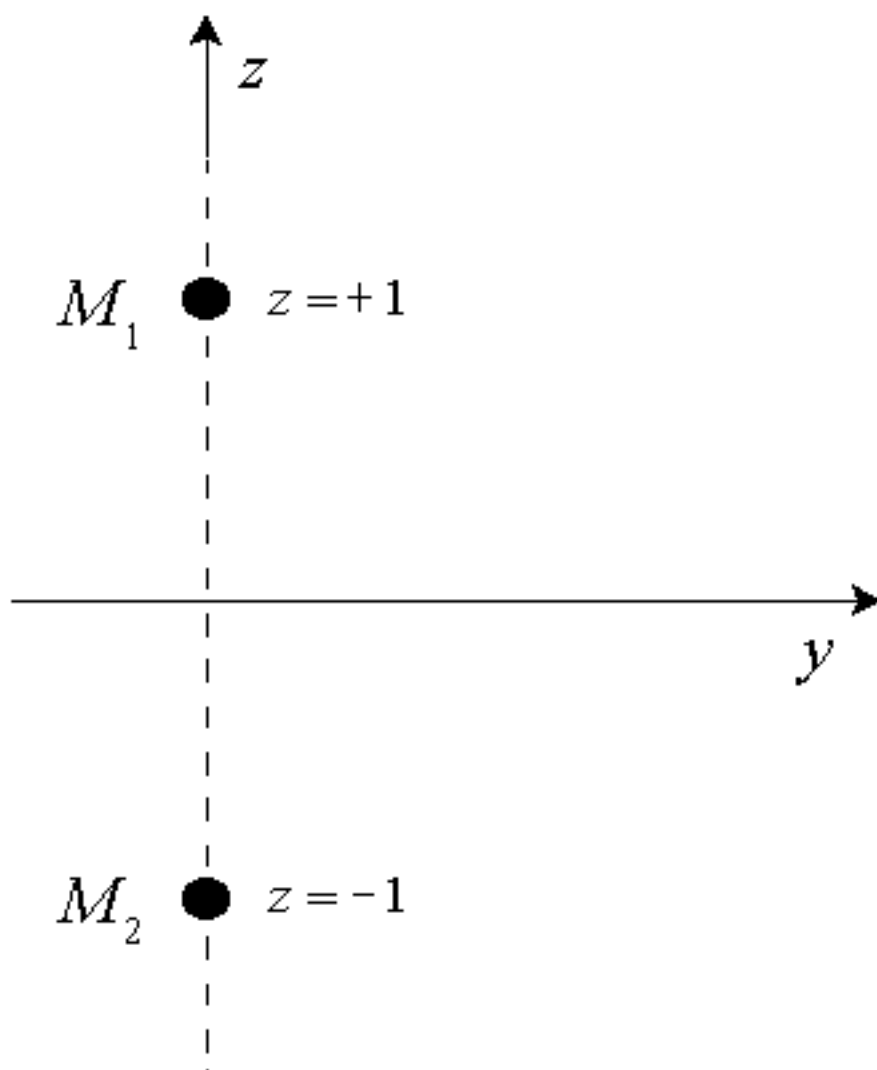
Figure 6. Construction of the compact set $D \subset \mathcal{S}$ used in defining the compact future-invariant subset $\Lambda \subset T_1^*\mathcal{S}$ [see Eq. (29)]. The circles \mathcal{C} and \mathcal{C}_i are chosen large enough so that any geodesic crossing them in the outward direction never comes back (it escapes to the corresponding asymptotic infinity). The subset D is the compact connected region bounded by the three circles.

Figure 7. Closed (or almost closed) orbits in the geodesic flow on (\mathcal{S}, h) . The top four plots are drawn with unit masses $M_1 = M_2 = 1$, and the two plots at the bottom of the figure are drawn with masses $M_1 = 2$ and $M_2 = 1$. As the orbits get more complicated (and therefore their periods become longer), numerical instabilities set in as soon as or before the full shape of the orbit

becomes apparent (as happens in the middle two plots). Recall that all these orbits are unstable because of the negatively curved geometry of (S, h) .

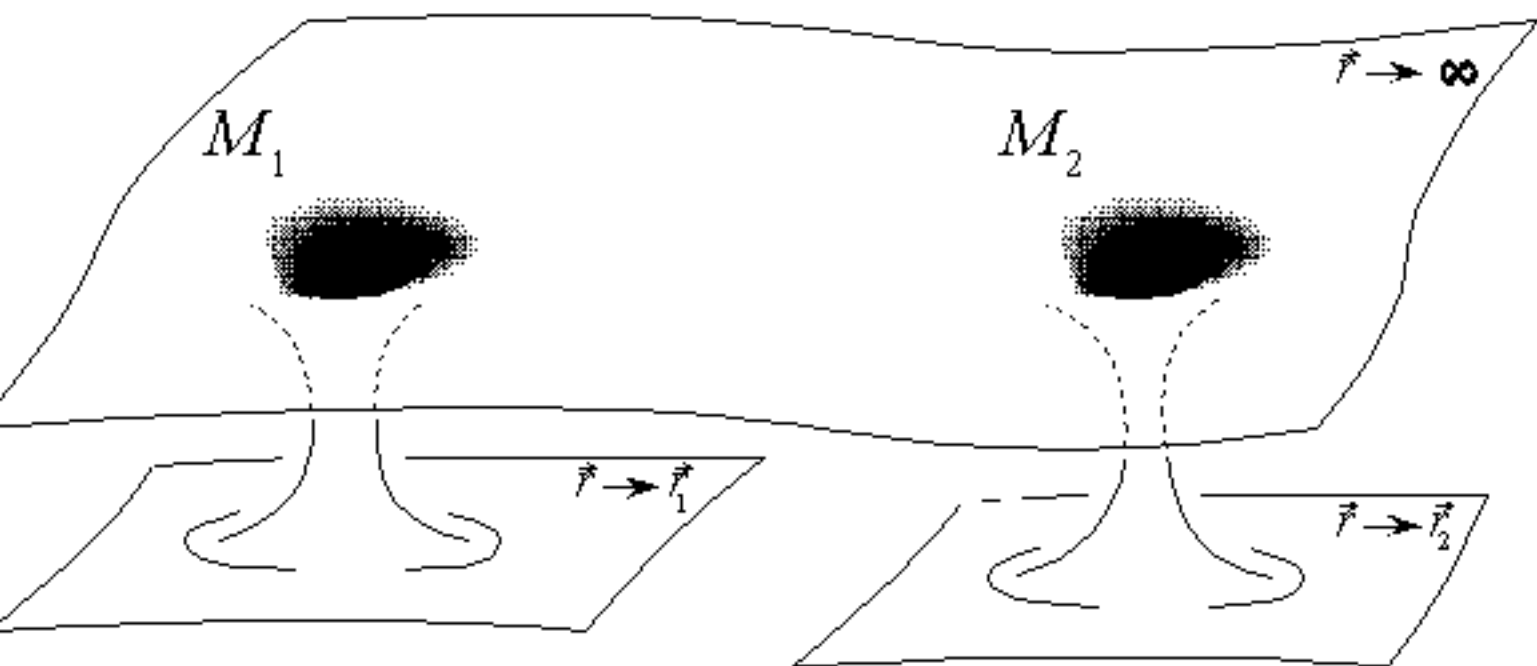
This figure "fig1-1.png" is available in "png" format from:

<http://arxiv.org/ps/gr-qc/9412031v1>



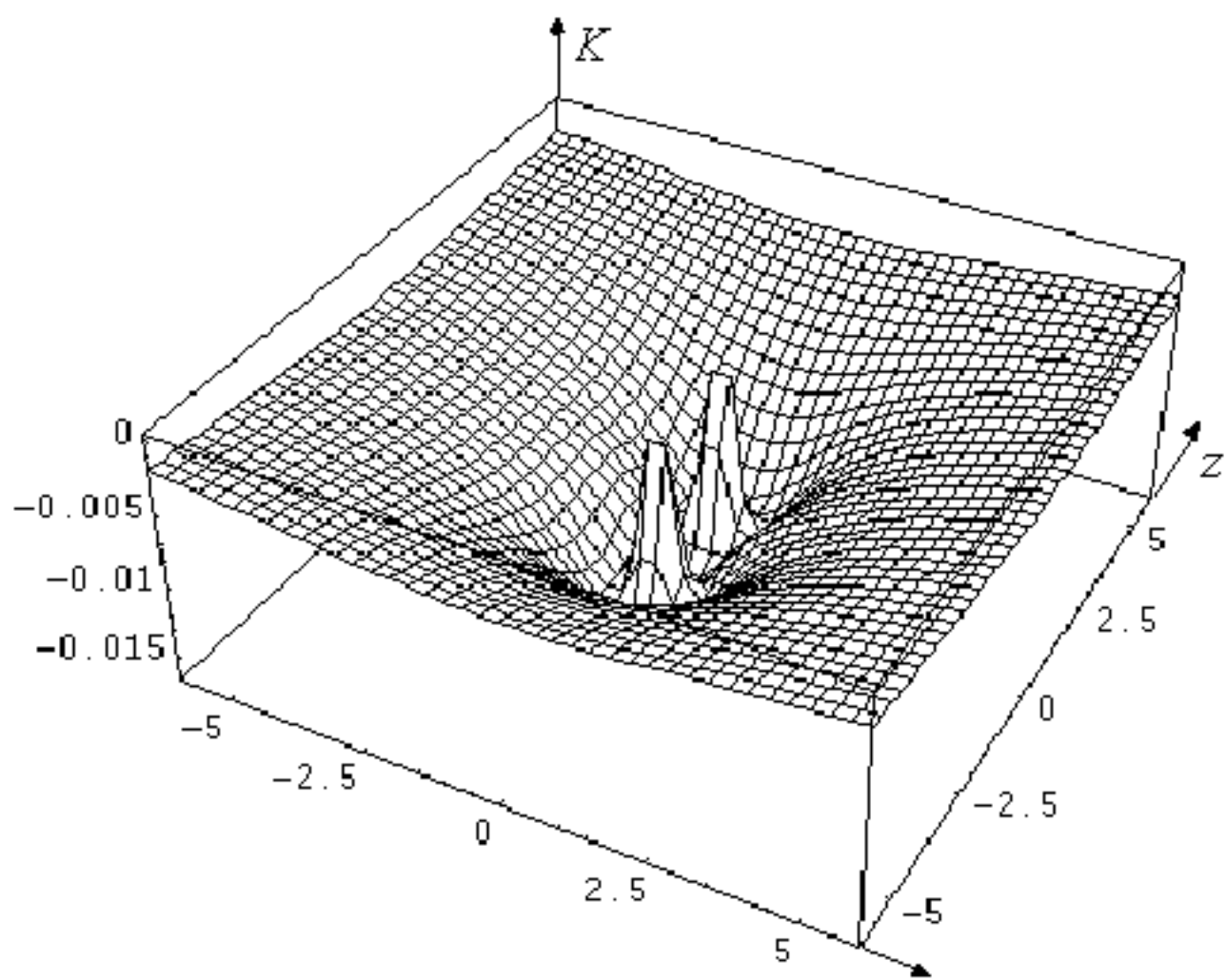
This figure "fig1-2.png" is available in "png" format from:

<http://arxiv.org/ps/gr-qc/9412031v1>



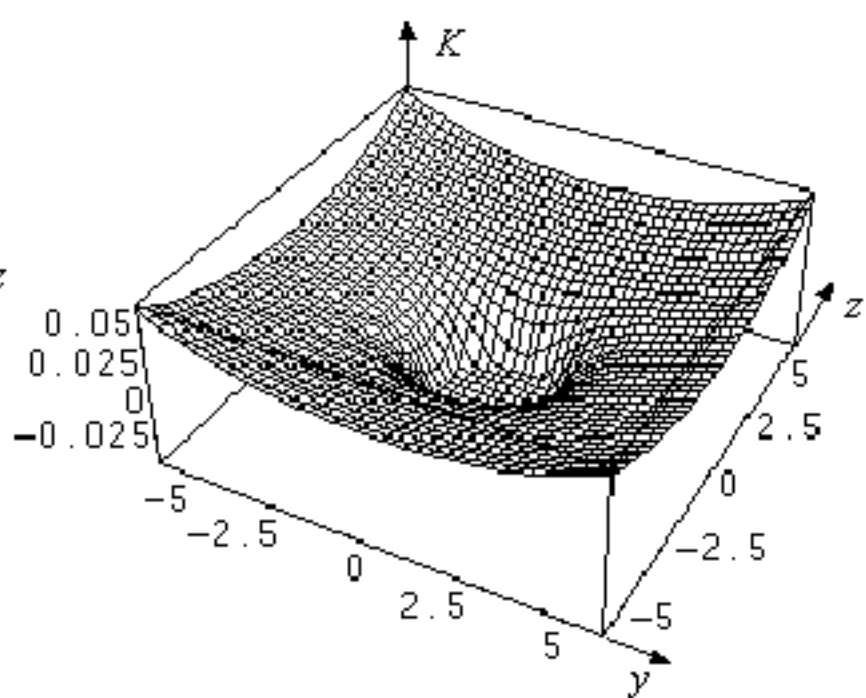
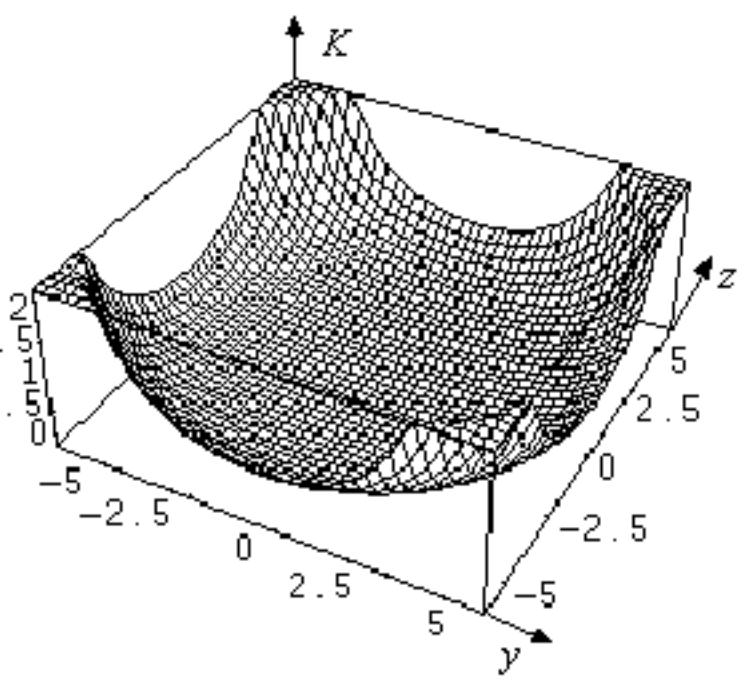
This figure "fig1-3.png" is available in "png" format from:

<http://arxiv.org/ps/gr-qc/9412031v1>



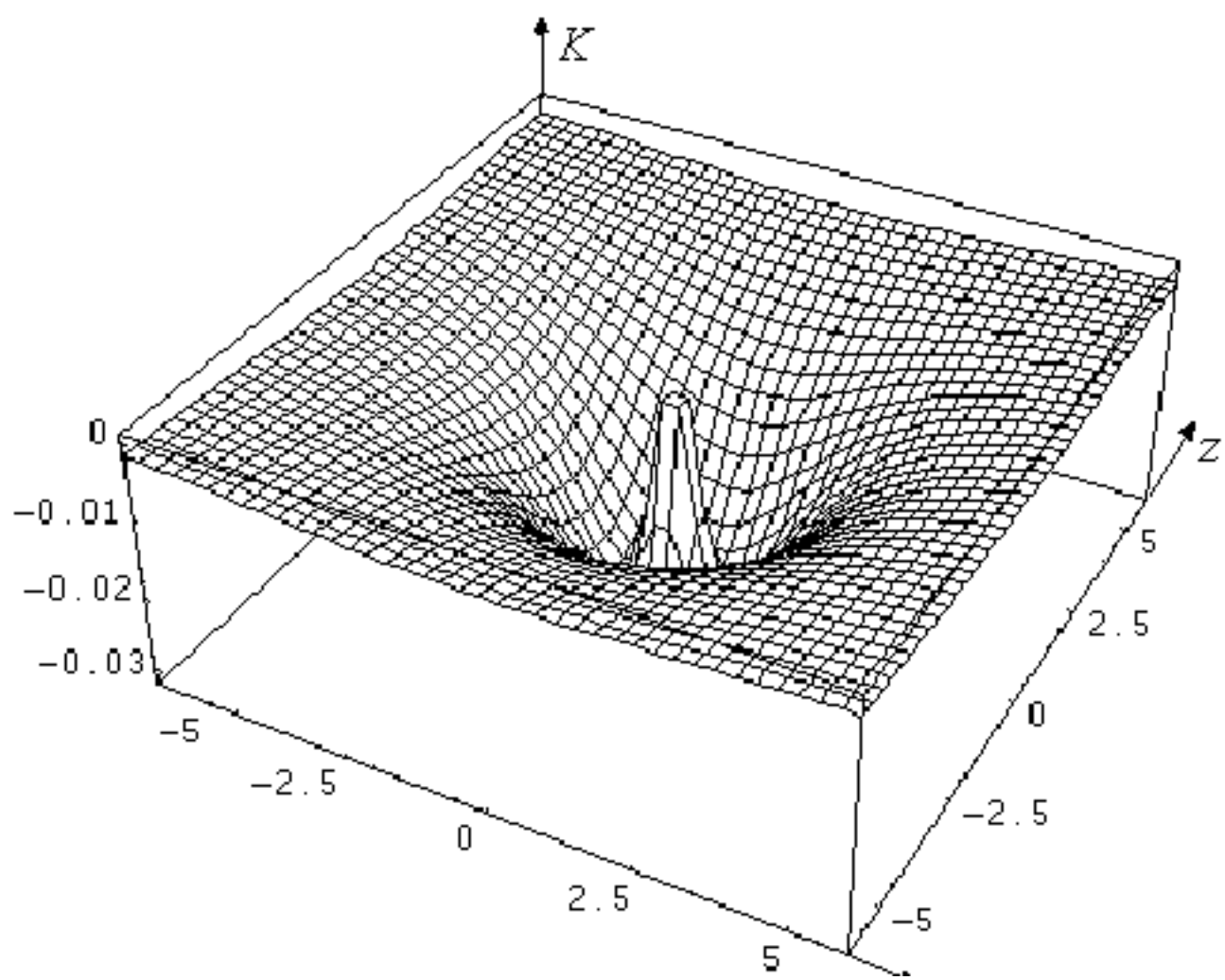
This figure "fig1-4.png" is available in "png" format from:

<http://arxiv.org/ps/gr-qc/9412031v1>



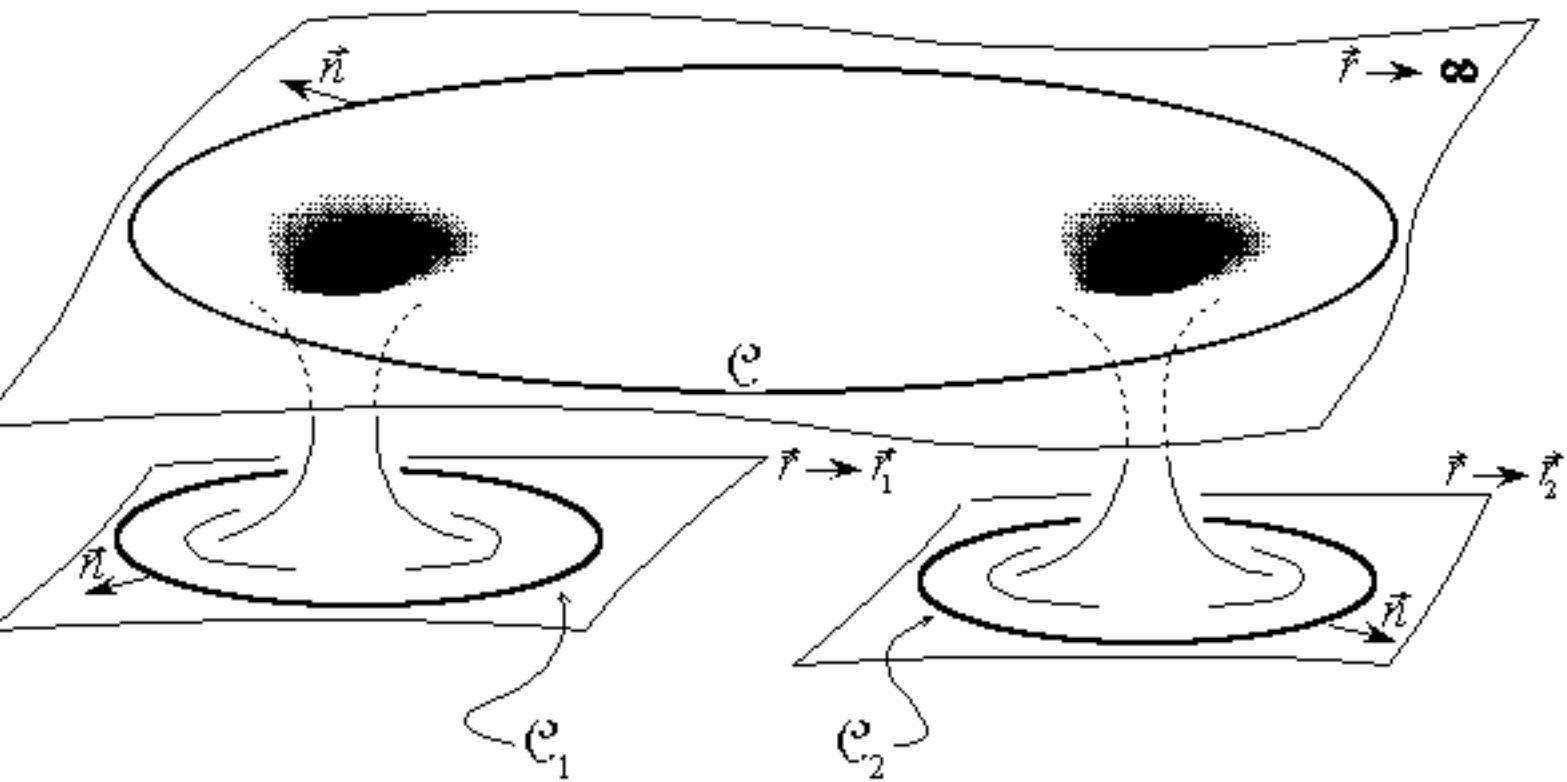
This figure "fig1-5.png" is available in "png" format from:

<http://arxiv.org/ps/gr-qc/9412031v1>



This figure "fig1-6.png" is available in "png" format from:

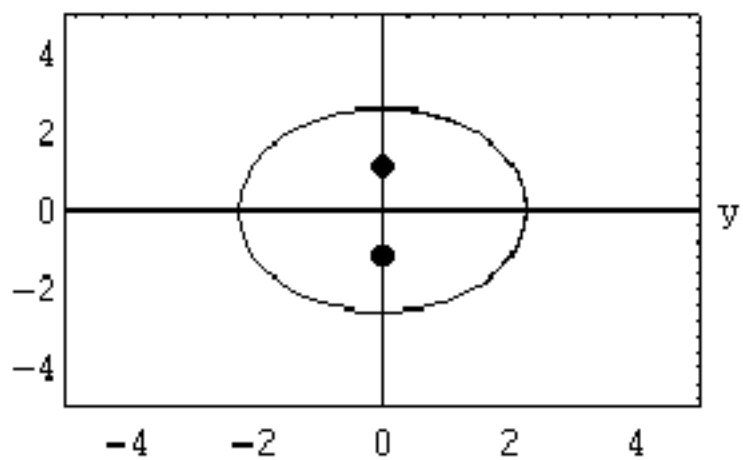
<http://arxiv.org/ps/gr-qc/9412031v1>



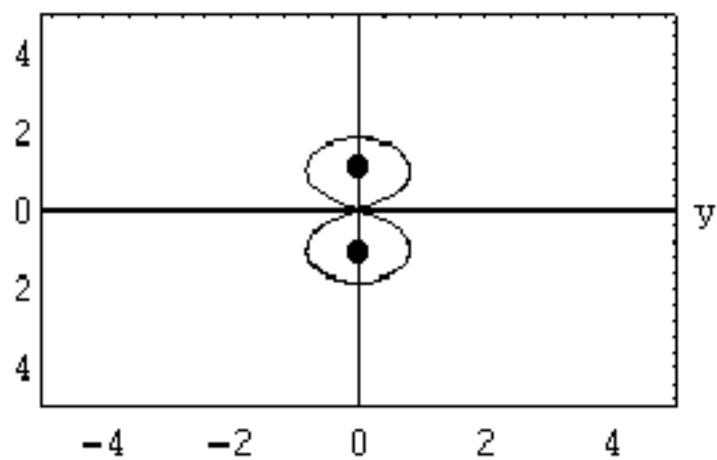
This figure "fig1-7.png" is available in "png" format from:

<http://arxiv.org/ps/gr-qc/9412031v1>

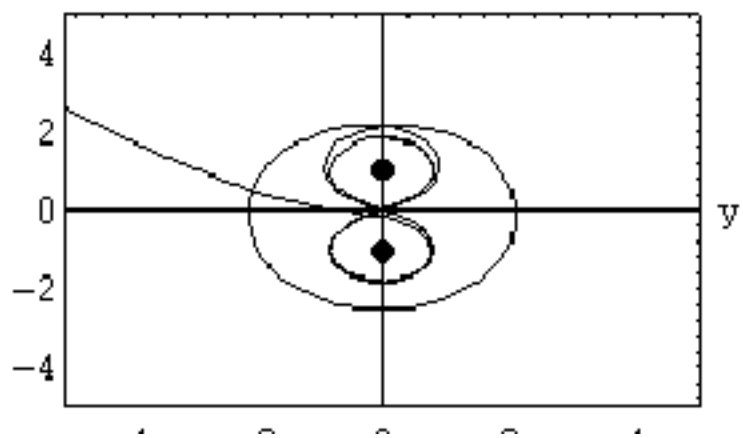
z



z



z



z

